

# **Gel–glass transition in silica and nitrated silica aerogels – experiment and computer modelling**

KRYSZYNA SZANIAWSKA<sup>1</sup>, LEON MURAWSKI<sup>1</sup>, JAROSŁAW RYBICKI<sup>1</sup>, AGNIESZKA WITKOWSKA<sup>1</sup>,  
MACIEJ WALEWSKI<sup>2</sup>

<sup>1</sup>Faculty of Applied Physics and Mathematics, Technical University of Gdańsk,  
ul. Gabriela Narutowicz 11/12, 80–952 Gdańsk, Poland.

<sup>2</sup>Faculty of Chemistry, Technical University of Gdańsk, ul. Gabriela Narutowicza 11/12, 80–952 Gdańsk,  
Poland.

Nitrated silica aerogel was sintered at 1600 °C in vacuum or nitrogen atmosphere and the effect of densification was compared with that observed in silica aerogel. It has been shown that homogeneous oxynitride glasses containing 8.4–13 wt% can be obtained by densification of nitrated aerogels. The densification process of nitrated aerogels was simulated by computer modeling using classical molecular dynamics (MD) simulations. MD simulations have shown that densification process proceeds in a similar way as in the experiment. In addition, the simulations indicate that oxynitride glasses can be obtained by densification of Si–O–N system.

Keywords: sol-gel method, aerogels, silica, nitridation, molecular dynamics simulations.

## **1. Introduction**

The sol-gel method is an alternative approach to the production of monolithic glasses. It is a well-known fact that during the drying and densification processes in xerogels, shrinkage and cracking caused by capillary forces usually make it difficult to obtain large pieces of glass. One method to prevent cracking is to dry wet gel under hypercritical conditions, which leads to the formation of a porous solid known as an aerogel. The aerogels as porous bodies are sintered by means of a viscous flow causing the collapse of pores and coalescence of solid particles [1], [2]. The driving force for this process is supplied by the interfacial energy, which permits to sinter aerogels at low temperature [3].

Aerogels have very high porosity exceeding 95% and also a large specific surface area. These properties are very useful for their structural modifications. Recently, we have found that more than 30 wt% of nitrogen can be incorporated in silica aerogels during ammonolysis. In addition, some of the nitrated aerogels were densified to the monolithic oxynitride glasses [4], [5]. In the present paper we discuss the gel–glass transition in silica and nitrated silica aerogels. We compare the experimental observations with the results of MD simulation.

## 2. Experimental

Homogenous  $\text{SiO}_2$  gels were prepared by hydrolysis and polycondensation of tetraethoxysilane (TEOS) in an alcohol solution. Details of this procedure were presented in our previous paper [4]. Drying of the gels was performed under supercritical conditions for ethanol (243 °C, 65 bar) by applying an inert gas ( $\text{N}_2$ ) pressure in an autoclave. Gel–glass conversions were performed in air by heating aerogels with a heating rate 600 °C/h from room temperature to 900 °C and afterwards with 300 °C/h to the final temperature 1200 °C. For ammonolysis the silica aerogels were exposed to reaction with ammonia in a silica glass tube furnace under  $\text{NH}_3$  gas at 1200 °C. Nitrided aerogels were sintered at 1600 °C in vacuum. The heating rate was 17 °C/min up to the temperature 1100 °C and then 5 °C/min to the final temperature (1600 °C). This temperature was kept unchanged for 1 h. After that the furnace was cooled down rapidly. That process produced fully dense and transparent glasses.

The specific surface area and pore size distribution of aerogels were measured by the nitrogen adsorption-desorption technique using Brunauer–Emmet–Teller isotherm (BET). X-ray diffraction patterns of aerogels and glasses show that all the samples were amorphous. The nitrogen content of nitrided aerogels and glasses was determined chemically using the method of GUYADER *et al.* [6].

## 3. Results and discussion

### 3.1. Densification of silica aerogels

Densification process of silica and multicomponent gels has been discussed by BRINKER *et al.* [7], [8]. They propose four mechanisms that are operative during gel–glass conversion: capillary contraction, condensation polymerization, structural relaxation, and viscous sintering. Silica aerogels are characterized by an “open” texture

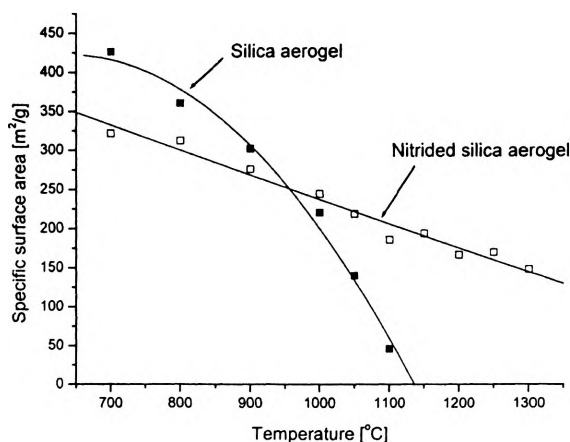


Fig. 1. Specific surface area vs. heat treatment temperature for aerogel heated in air (■) and in flowing ammonia (□). The solid lines are guide for eye.



(> 90% porosity) and by low density ( $< 0.2 \text{ g/cm}^3$ ); they are also hydrophobic. These properties make aerogels different in behaviour from typical xerogels densified in air. WOIGNIER *et al.* [3] have shown that mainly two kinds of mechanisms are responsible for the sintering. At low temperatures (from 500 to 700 °C) the sintering is by a diffusional process. In this temperature range, material weight losses are important. The observed shrinkage is due to the coalescence of gel particles as a consequence of thermal condensation of silanol groups. In the temperature range 700–1000 °C (see Fig. 1) a large decrease in the surface area is observed and in the sintering two mechanisms coexist: diffusional process and viscous flow. Above 1000 °C only a viscous flow phenomenon takes place. As shown in Fig. 1, full densification is accomplished in a narrow temperature range. Glasses obtained in this way are dense, transparent and exhibit the same physical properties as molten silica.

### 3.2. Densification of nitrated aerogels

In a previous work [5], we have shown that silica aerogels can be nitrated by ammonia treatment at the range of temperatures from 700 to 1300 °C. We have found that the amount of nitrogen incorporated in silica aerogel depends on the final temperature of ammonolysis and on the time of heat treatment. The specific surface area of nitrated aerogels remains high and decreases with the temperature of ammonolysis and with nitrogen content. A typical aerogel has a surface area between 400–500  $\text{m}^2/\text{g}$  and the maximum of pore size distribution between 50–70 nm [4]. For a typical nitrated aerogel containing from 10 to 20 wt% of nitrogen some shrinkage is observed after nitridation. The surface area decreases about 100  $\text{m}^2/\text{g}$  (Fig.1) and pore size distribution is shifted to smaller pores with the maximum between 30–40 nm (see Fig. 2). These aerogels can be easily converted to dense oxynitride glasses by heating at 1600 °C in vacuum or nitrogen atmosphere. As shown in Tab. 1, during gel to glass conversion the nitrogen content decreases to 8.4–13.0 wt% for aerogels containing 10.0–16.8 wt% nitrogen prior to sintering.

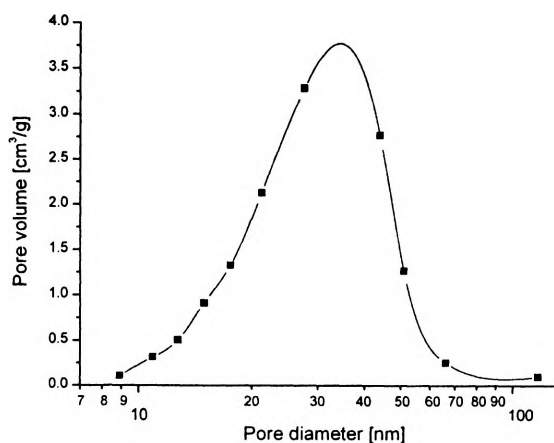


Fig. 2. Pore size distribution for nitrated aerogel containing 16.83 wt% N. The solid line is guide to eye.



Table 1. Nitrogen content (wt%) in nitrated aerogel and oxynitride glasses.

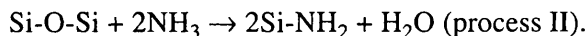
Aerogel [wt% N]	10.0	12.7	15.4	16.8	19.0	21.1	24.6	28.7
Results of sintering [wt% N]	8.4	9.5	9.6	13.0	*	*	*	*
	glass	glass	glass	glass	glass	evaporated	evaporated	evaporated

\* wt% of N was not determined.

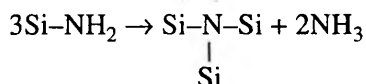
The mechanism of the incorporation of nitrogen into the silica aerogel is complicated, because it is necessary to consider the numerous reactions and processes which can occur between ammonia and the porous network. Several reactions between ammonia and silica aerogel can be proposed to account for this mechanism [9], [10]. For example, at low temperatures, amine species may form due to interactions between ammonia and silanol groups:



or with siloxane bonds



With increasing treatment temperature, the process II becomes dominant and at high temperatures (> 1000 °C) the resultant Si-NH<sub>2</sub> groups condense to form nitrides according to the reaction:



According to these reactions, a two-coordinated oxygen is replaced by a three-coordinated nitrogen in the aerogel structure. Consequently, the reduction in BET surface area occurs (Fig. 1). We have observed that 15–37 wt% nitrogen escaped from the aerogel during densification (see Tab. 1). This indicates that a large portion of the nitrogen is incorporated in the aerogel to form Si-N bonds.

Some differences are observed when the densification processes of aerogels in air and in ammonia are compared (Fig. 1). In nitrated aerogel during densification in an ammonia atmosphere, the first reaction can be attributed to the condensation of amines. At higher temperatures and in strongly reducing atmosphere the nitridation is enhanced. Therefore, it is impossible to obtain fully densified glass during heat treatment in ammonia. In addition, nitrogen in three-fold coordination serves as a cross-linking agent which should raise the glass-transition temperature and the required sintering temperature of a nitrated aerogel. As it was mentioned before, full densification of nitrated aerogel was obtained by heat treatment at 1600 °C in vacuum or in a nitrogen atmosphere. An important result is that aerogel-glass conversion proceeds in the same way as in silica aerogels. We believe that similar processes take place during densification. The only difference is that the condensation of amines



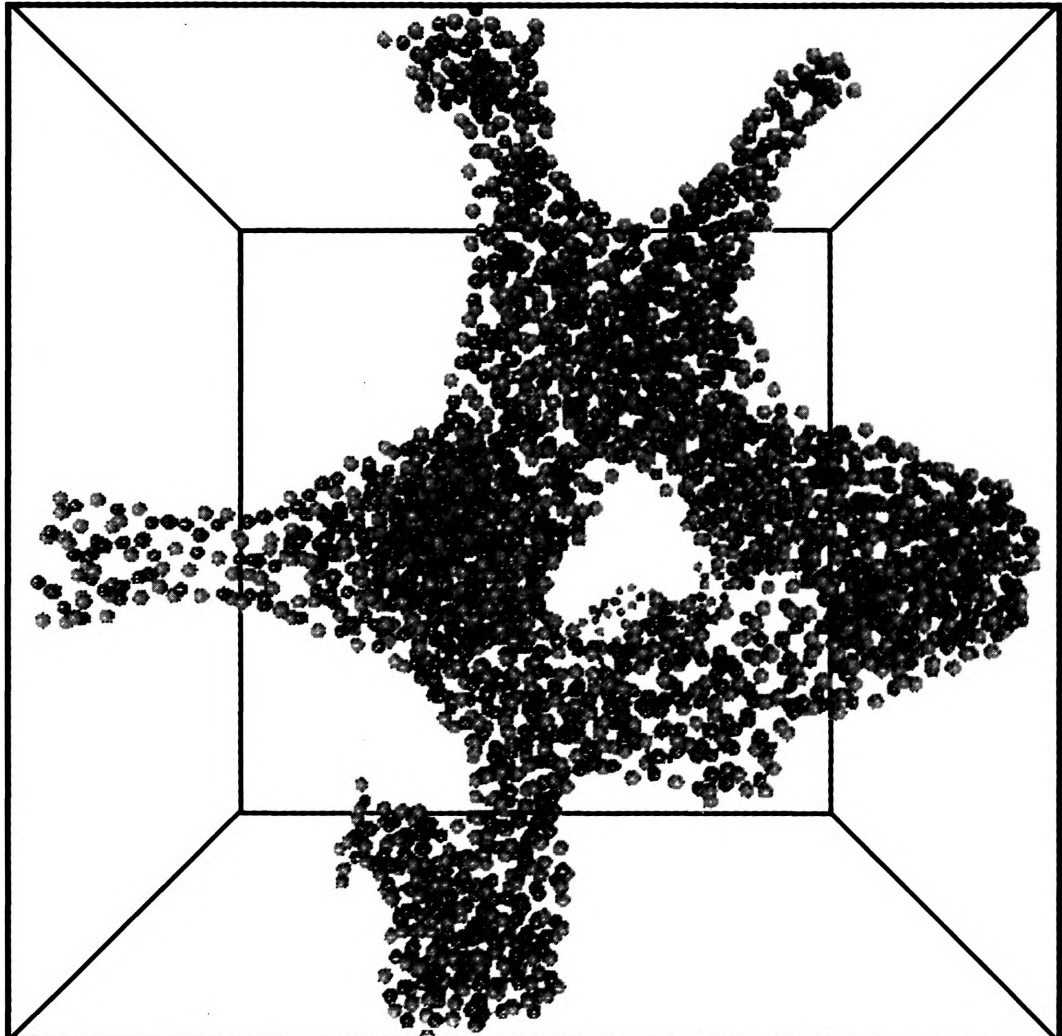


Fig. 3. Atomic configuration in the last time-step of the simulation for  $\text{Si}_5\text{N}_2\text{O}_7$ .

should be taken into account for diffusional processes. Because the nitrated aerogels contain three coordinated nitrogen, a viscous flow occurs at higher temperatures. It is not clear why aerogels containing more than 20 wt% of nitrogen were evaporated during heat treatment (see Tab. 1). We suppose that for these aerogels a different procedure of heat treatment should be applied.

#### 4. Molecular dynamics simulations

Densification process of nitrated aerogels was simulated by computer modeling. Classical MD simulations of three systems ( $\text{Si}_5\text{N}_2\text{O}_7$ ,  $\text{Si}_{10}\text{N}_6\text{O}_{11}$  and  $\text{Si}_5\text{O}_4\text{N}_4$ ) have been performed. These systems correspond to nitrated aerogels containing 10.0, 15.5 and 21.5 wt% of nitrogen. The numbers of atoms within the simulation box are listed in Tab. 2. The calculations have been realised in the microcanonical (NVE), and isothermal-isobaric (NpT) ensembles (e.g., [11]) for simulations of gel structure and gel spontaneous densification, respectively. The atoms were assumed to interact by a two-body potential (Born–Mayer repulsive forces, and Coulomb forces due to ionic charges, calculated with the aid of the standard Ewald technique). The Si–Si, N–N and O–O interaction parameters were taken from [12]. The cross-interaction parameters (i.e., for pairs Si–O, Si–N and N–O) were calculated as suitable averages of the Si–Si, N–N and O–O parameters using the Lorenz–Berthelot mixing rule [11]. Initial atom configurations were skew-started at low density of  $200 \text{ kg/m}^3$ , common for all compounds considered, with partial ionic charges equal to 10% of the full ionic charge. The latter trick was applied to mimic charge screening by the solvent which was not

Table 2. Numbers of atoms in the simulation boxes.

	Si	O	N
$\text{Si}_5\text{O}_7\text{N}_2$	1000	1400	400
$\text{Si}_{10}\text{O}_{11}\text{N}_6$	1000	1100	600
$\text{Si}_5\text{O}_4\text{N}_4$	1000	800	800

simulated itself. The initial configurations were thermalised, and then the Vashishta algorithm was applied to restore full ionic charges (during 400,000 time-steps  $\Delta t$ ,  $\Delta t = 10^{-15}$  s). The final low density configurations obtained in the NVE conditions were submitted to spontaneous densification by switching on the NpT algorithm, i.e., simply allowing the variations of the simulation box volume. The results of our preliminary simulations can be summarised as follows.

For each low (fixed) density sample a similar porous structure has been obtained. Figure 3 shows the atomic configuration in the last time-step of the simulation for one of the samples. As it is seen, the obtained low density material has gel-like porous structure (note periodic boundary conditions applied in the simulations).

If the simulation box volume is allowed to vary (at zero external pressure), the samples spontaneously collapsed. Figure 4 shows the system density vs. time,



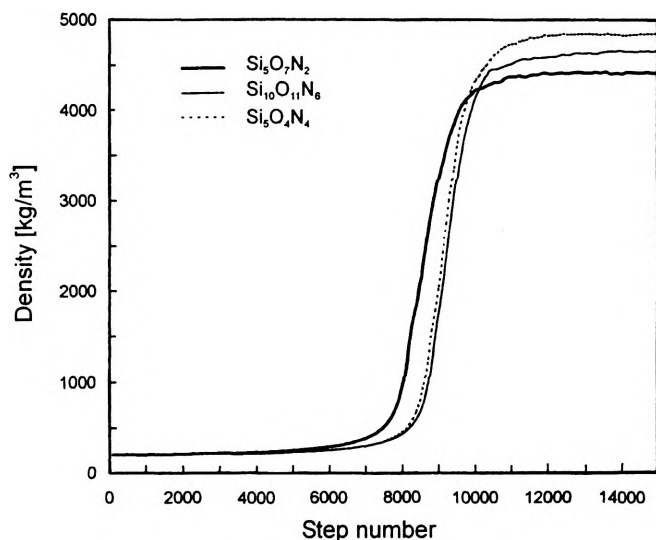


Fig. 4. System densities vs. time, measured from the beginning of the NpT runs.

T a b l e 3. Si–O, Si–N co-ordination number in low and high density phases.

		Si–O	Si–N
Si <sub>5</sub> O <sub>7</sub> N <sub>2</sub>	Gel	3.7	1.2
	Densified gel	4.9	1.4
Si <sub>10</sub> O <sub>11</sub> N <sub>6</sub>	Gel	3.0	1.8
	Densified gel	4.1	2.0
Si <sub>5</sub> O <sub>4</sub> N <sub>4</sub>	Gel	2.1	2.4
	Densified gel	3.0	2.8

measured from the beginning of the NpT runs. It is shown that similar to the experimental observation, densification process occurs during a short time. In order to characterise the differences between bulk glasses and gels, in Tab. 3 we give the first co-ordination numbers of Si ions.

## 5. Conclusions

The nitrated aerogels can be converted to dense homogeneous oxynitride glasses by heat treatment at 1600 °C in vacuum or in a nitrogen atmosphere. After the gel-to-glass conversion the nitrogen contents were 13.0–8.4 wt% for aerogels containing 16.8–10 wt% nitrogen before sintering. MD simulations have shown that the densification process of similar systems proceeds in the same way as it is observed in the experiment. In addition, the present MD simulations confirm that oxynitride glasses can be obtained by densification of Si–O–N system.

## References

- [1] BRINKER C.J., SCHERER G.W., *Sol-Gel Science*, Academic Press, New York 1990, Chap. 3.
- [2] PRASSAS M., PHALIPPOU J., ZARZYCKI J., *J. Mater. Sci* **19** (1984), 1656.
- [3] WOIGNIER T., PHALIPPOU J., PRASSAS M., *J. Mater. Sci.* **25** (1990), 3118.
- [4] SZANIAWSKA K., MURAWSKI L., PASTUSZAK R., WALEWSKI M., *Opt. Appl.* **30** (2000), 529.
- [5] SZANIAWSKA K., MURAWSKI L., PASTUSZAK R., WALEWSKI M., FANTOZZI G., *J. Non-Cryst. Solids* **286** (2001), 58.
- [6] GUYADER J., GREKOV F.F., MARCHAND R., LANG J., *Rev. Chim. Miner.* **15** (1978), 431.
- [7] BRINKER C.J., SCHERER G.W., ROTH E.P., *J. Non-Cryst. Solids* **72** (1985), 345.
- [8] SCHERER G.W., BRINKER C.J., ROTH E.P., *J. Non-Cryst. Solids* **72** (1985), 369.
- [9] KAMIYA K., OHYA M., YOKO Y., *J. Non-Cryst. Solids* **83** (1986), 208.
- [10] UNUMA H., YAMAMOTO M., SUZUKI Y., SAKKA S., *J. Non-Cryst. Solids* **128** (1991), 223.
- [11] RAPAPORT D.C., *Art of the Molecular Dynamics Simulation*, University Press, Cambridge 1995.
- [12] ABRAHAMSON A.A., *Phys. Rev.* **178** (1969), 76.

Received September 26, 2002